JOURNAL OF MATERIALS SCIENCE 29 (1994) 2611–2619

Carbothermal formation of β′-sialon from kaolinite and halloysite studied by ^{29}Si and ^{27}Al solid state MAS NMR

K. J. D. MACKENZIE, R. H. MEINHOLD, G. V. WHITE, C. M. SHEPPARD
New Zealand Institute for Industrial Research and Development, P.O. Box 31-310, Lower Hutt, New Zealand

B.L. SHERRIFF
Department of Geological Sciences, University of Manitoba, Winnipeg, Manitoba, Canada R3T 2NZ

^{27}Al and ^{29}Si magic-angle spinning (MAS) nuclear magnetic resonance (NMR) and complementary X-ray diffraction (XRD) studies of carbothermal formation of sialons from kaolinite and halloysite confirm that the reaction involves the initial formation of mullite ($3Al_2O_3 \cdot 2SiO_2$) and amorphous silica. In the presence of carbon, Si–N bonds are formed at ≈1200 °C, giving a continuum of silicon oxynitride compositions which become progressively more N-rich. These do not become sufficiently ordered to be detected by XRD until later in the reaction, when crystalline silicon oxynitride, possibly containing a little Al (O′-sialon) and *x*-phase sialon are formed, followed by β′-sialon. The O′- and *x*-phase sialons are transitory, but the β′-sialon persists throughout the reaction. Si–O bonds survive the destruction of the mullite and persist throughout the reaction, especially with kaolinite starting material. The ^{29}Si MAS NMR results indicate that Si–C bonds are formed later in the reaction than previously suggested, the SiC phase behaving more like a secondary product than a transitory intermediate. Al–N bonds are not detectable by ^{27}Al MAS NMR until very late in the reaction (after 8 h firing at 1400 °C), and coincide with the appearance of the secondary product AlN. The implications for the carbothermal reaction sequence in kaolinite and halloysite are discussed.

1. Introduction

The generic term "sialon" covers a range of oxynitrides of silicon and aluminium, which can have widely varying compositions and a number of different structural types. Many of these compounds find applications as high technology ceramics, for wear parts, cutting tools or special-purpose refractories. The β′-series of sialons, which are isostructural with β-Si_3N_4 have been the most extensively exploited so far. These have the general formula

$$Si_{6-z}Al_zO_zN_{8-z}$$

where z can vary from 0 (corresponding to Si_3N_4) up to about 4.3.

Of the number of methods available for the synthesis of β′-sialon, carbothermal reduction of aluminosilicate minerals, accompanied by simultaneous nitridation has the attraction of low raw materials costs. Carbothermal production of sialon has been demonstrated from kaolinite [1], halloysite [2, 3], pyrophyllite [4] and montmorillonite [5].

Carbothermal reduction of clay minerals such as kaolinite involves a complex sequence of reactions, of which the most important steps are [3, 6]:

(a) Thermal breakdown of the clay into mullite and silica (cristobalite) at about 1300 °C.

$$3Al_2Si_2O_5(OH)_4 \rightarrow \underset{\text{mullite}}{3Al_2O_3 \cdot 2SiO_2} + 4SiO_2 + 6H_2O \quad (1)$$

(b) Conversion of the silica to silicon carbide at 1300–1400 °C

$$4SiO_2 + 12C \rightarrow 4SiC + 8CO \quad (2)$$

(c) Reaction of silicon carbide with mullite and nitrogen forming the highly aluminous *x*-phase sialon which further reacts to form β′-sialon

$$\underset{\text{mullite}}{3Al_2O_3 \cdot 2SiO_2} + SiC + N_2 \rightarrow \underset{x\text{-phase sialon}}{Si_3Al_6O_{12}N_2} + CO \quad (3)$$

$$\underset{x\text{-phase sialon}}{Si_3Al_6O_{12}N_2} + 3SiC + 3C + 4N_2 \rightarrow \underset{\beta'\text{-sialon}}{2Si_3Al_3O_3N_5} + 6CO \quad (4)$$

The β′-sialon is not necessarily the final sialon product; further reaction can result in the removal of Si and O, forming 15R sialon [3], one of several polytypoid

0022–2461

phases with layer structures related to AlN, of general formula $Si_{6-x}Al_{x+y}O_xN_{y+8-x}$.

During the course of this reaction sequence, other phases may also be formed, depending on the impurity content of the starting materials or the processing conditions. Thus, the presence of iron impurities which facilitate SiC formation, also promotes the formation of Si_3N_4 and Al_2O_3 at the expense of sialon [3]. The formation of Si_3N_4 can be suppressed by low nitrogen flow rates which help to maintain higher CO concentrations over the reactant bed [7].

Although X-ray powder diffraction continues to be the primary technique for investigating these reaction sequences, ^{29}Si and ^{27}Al solid-state NMR with magic-angle spinning (MAS NMR) has recently proved capable of providing useful complementary information about related thermal reactions in clay minerals [8]. The ^{29}Si and ^{27}Al NMR spectra have also been reported for a number of phases encountered in the reaction sequence (Table I), and a brief study has indicated the potential of MAS NMR in following the progress of sialon formation in halloysite [9], and for shedding light on the intermediates formed during the formation of β′-sialon from organosilicon polymers [10]. The present paper reports a ^{29}Si and ^{27}Al MAS NMR study of the carbothermal reaction sequence of kaolinite and halloysite to form sialon.

TABLE I Previously reported ^{29}Si and ^{27}Al MAS NMR chemical shifts for the various phases likely to be encountered in the carbothermal reduction of kaolinite. ^{29}Si chemical shifts quoted with respect to TMS, ^{27}Al shifts referenced to $Al(H_2O)_6^{3+}$. Resonances listed in decreasing order of intensity

Phase	Chemical shift (p.p.m.)	References
^{29}Si		
Mullite	− 86	11
Mullite	− 87.5, − 91 to − 94	12
Mullite	− 86.8, − 90(sh), − 94.2	13
α-SiC	− 13.9 to − 14.9, − 20.2 to − 20.8, − 24.1 to − 24.9	14, 15, 16
β-SiC	− 16.1 to − 18.5	14, 15, 16, 17
β′-sialon	− 48	18
β′-sialon	− 47.6 to − 48.4	23
O′-sialon	− 60.9 to − 61.5, − 48.4 to − 48.9	23
AlN polytypoid	− 48.1, − 36	19
AlN polytypoid	− 49, − 30 to − 35	20
α-Si_3N_4	− 47 to − 48, − 48 to − 49.7	18, 20
α-Si_3N_4	− 46.4, − 47.3, − 48.1	17
β-Si_3N_4	− 48.4 to − 49	17, 18, 20
Si_2N_2O	− 63	18
^{27}Al		
Mullite	48, − 8	12
Mullite	42.2–48.3, 56.6–66.1, 3.5 to − 9.1	13
x-phase sialon	66.9, 0.8	19
β′-sialon	66, 103–109, 4	21
β′-sialon	69.1, 106.6–112.5, − 6.6–10	23
O′-sialon	64.7, 2.3	23
AlN polytypoid	108.2–110, 0–13	19, 20, 22
AlN	113	21
Al_5O_5N (approx.)	12, 65, 114	21

2. Experimental procedure

The clay starting materials were BDH (British Drug Houses) "light" kaolinite and New Zealand China Clays halloysite, with chemical compositions as shown in Table II. X-ray powder diffraction shows both clays to be reputable, well crystallized materials, with the additional SiO_2 content of the halloysite present as cristobalite.

Reaction mixtures containing 25 wt % carbon (Degussa lampblack 101) were ball-milled in hexane for 17 h using ZrO_2 balls to minimize iron contamination as far as possible. The mixture was then extruded into 2 mm diameter rods and fired in small alumina crucibles in a laboratory electric tube furnace at temperatures ranging from 1100 to 1400 °C for 10 min, and at 1400 °C for times ranging from 10 min to 24 h. The firing atmosphere was oxygen-free nitrogen (flow rate 150 ml min^{-1}), further purified by passing through a catalytic converter. After cooling under nitrogen, the samples were crushed and examined by X-ray powder diffraction using a Philips PW1700 computer-controlled diffractometer with CoK_α radiation and a graphite monochromator. In addition to the identification of the phases present, semi-quantitative estimates of their relative concentrations were made from the peak heights of the following X-ray reflections: mullite (JCPDS file No. 15–776), 0.34 nm; β′-sialon (25–1492), 0.666 nm; O′-sialon (33–1162), 0.444 nm; x-phase sialon (35–23), 0.364 nm; cristobalite (11–695), 0.407 nm; AlN (25–1133), 0.270 nm; β-Si_3N_4 (33–1160), 0.266 nm; SiC (29–1129), 0.155 nm. These reflections represent the most intense peaks in all phases except β′-sialon and SiC, in which interference from other phases made it necessary to use a less intense peak, which was scaled to the major peak height for consistency. Small variations in the peak positions of β′-sialon and β-Si_3N_4 were observed, the

TABLE II Chemical composition of the clays used, by XRF (analyst: J. Hunt)

Element	Kaolinite (wt %)	Halloysite (wt %)
Al_2O_3	37.8	34.41
SiO_2	46.2	51.3
Fe_2O_3	0.45	0.14
TiO_2	0.03	0.09
CaO	< 0.01	< 0.01
MgO	0.35	< 0.04
K_2O	0.75	0.05
Na_2O	0.14	< 0.09
P_2O_5	0.21	0.11
LOI	13.14	13.34
Total	99.08	99.58

former due to changes in the z-value of the sialon during the reaction, the latter indicating the incorporation of some Al into the silicon nitride. For samples containing mullite, detailed measurements were made of the mullite unit cell dimensions, correcting the measured angular spacings by use of a silicon standard.

The ^{27}Al MAS NMR spectra were obtained at 11.7 T using a Bruker AMX 500 and a Varian Unity 500 spectrometer at a frequency of 130.3 MHz. A Doty high-speed MAS probe was used, at spinning speeds of up to 12.2 kHz and a 15° pulse of 1 μs with a recycle time of 1 s. The ^{29}Si spectra were obtained on the Unity 500 spectrometer at spinning speeds of about 8 kHz, with a 90° pulse and 300 s recycle time to accommodate the long relaxation times encountered in some of the sialon and carbide phases. The ^{27}Al chemical shifts were measured with reference to $AlCl_3$ in a 1 M aqueous solution, and the ^{29}Si shifts were referenced to tetramethylsilane (TMS).

3. Results and discussion

3.1. X-ray diffraction of phases formed in sialon reaction mixtures

The appearance and disappearance of the various phases in kaolinite and halloysite reacted in carbon with nitrogen under the present experimental conditions, based on the X-ray results, is shown semi-schematically in Figs 1 and 2, respectively.

The phase formed initially in both clays is mullite ($3Al_2O_3 \cdot 2SiO_2$), the concentration and crystallinity of which increases from 1100 °C (the lowest temperature

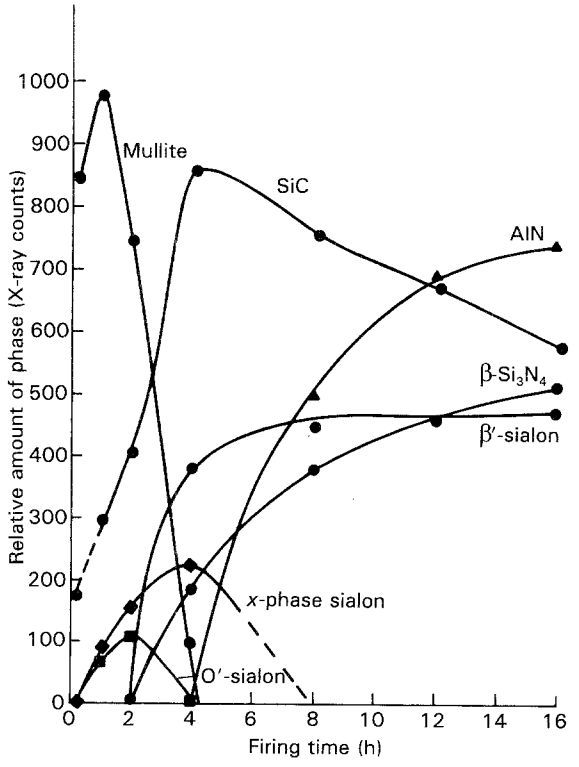

Figure 1 Semi-quantitative representation of the phases detected by XRD in kaolinite–carbon mixtures fired in nitrogen at 1400 °C for various times.

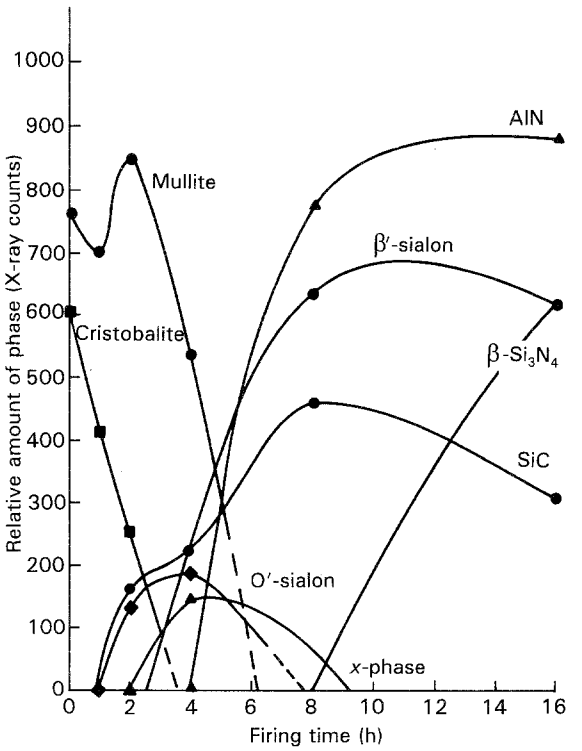

Figure 2 Semi-quantitative representation of the phases detected by XRD in halloysite–carbon mixtures fired in nitrogen at 1400 °C for various times.

samples studied here), reaching its maximum at the final reaction temperature of 1400 °C. The unit cell parameter of this mullite varied little above 1300 °C (the lowest temperature at which the phase was sufficiently crystalline for measurements to be made). From the relationship of Cameron [24], the compositions of these mullites were estimated to be 59–64 wt % Al_2O_3, in the range of the normal 3 : 2 mullite composition.

No cristobalite was formed in any of the kaolinite samples; the cristobalite in the halloysite samples was present in the starting material, and was progressively consumed during the reaction (Fig. 2). A considerable amount of X-ray amorphous silica occurred in the early stages of the reaction, as evidenced by the pronounced curvature of the diffraction background which disappeared only after firing for 2 h at 1400 °C.

The mullite progressively disappears over the first 4–6 h of reaction at 1400 °C, with the concomitant formation of O′-sialon and x-phase sialon (Figs 1 and 2). The O′-phase is essentially a silicon oxynitride, which may have a small amount of added Al. Its composition can be written as $Si_{2-x}Al_xN_{2-x}O_{1+x}$, where x can typically range from 0.04 to 0.28 [23].

β′-sialon first appears a little later than the O′-phase, but is more persistent than either of the transitory O′- and x-phases, becoming the major sialon phase after about 8 h firing at 1400 °C. At longer reaction times, it too decreases slightly in concentration, with an increase in AlN (not an AlN polytypoid sialon as might have been expected) and silicon nitride, which probably contains a small amount of Al, on the basis of the slight shift observed in the 0.266 nm peak.

Silicon carbide could be confidently identified in halloysite only after 2 h reaction (Fig. 2), but in kaolinite there is clearer evidence of a small SiC diffraction feature at 0.155 nm after 10 min reaction (Fig. 1). Although the detection of silicon carbide in kaolinite reacted for 10 min could not be confirmed by NMR (see below), the delayed appearance of SiC in halloysite is consistent with the NMR findings, and is contrary to previous suggestions [6] that β-silicon carbide is one of the earliest phases to be formed. The amount of silicon carbide formed in kaolinite reaches a maximum after about 2 h reaction (Fig. 1), and rather later in halloysite (Fig. 2). Thereafter, the silicon carbide concentration decreases slowly with reaction time, but continues to be present in significant amounts over the timescale of the present experiments. The eventual fate of the additional silica in the halloysite is not clear from Fig. 2; it does not appear to contribute to silicon carbide formation, which is less marked in halloysite than in kaolinite, but may contribute directly to the greater amount of β′-sialon formed, or be removed in the vapour phase as SiO.No AlN polytypoid sialon or Al_2O_3 was observed under the present reaction conditions.

3.2. NMR spectroscopy of the reaction mixtures

3.2.1. ^{27}Al NMR

Typical ^{27}Al NMR spectra of halloysite samples carbothermally reacted at 1400 °C for various times are shown in Fig. 3.

The spectra of the kaolinite samples are essentially similar to those of halloysite. The samples fired at times up to 4 h show both an octahedral and a tetrahedral feature at 0–5 p.p.m. and 56–64 p.p.m. respectively. These spectra agree broadly with a recently published mullite spectrum [13], and confirm the X-ray observation of mullite as the sole crystalline phase in these samples. The octahedral peak shows marked asymmetry in all these samples, probably due to electric field gradient (EFG) effects on the spin 5/2 nucleus. Some asymmetry is also visible in the tetrahedral peak, and appears to be due to the presence of another resonance at about 45 p.p.m.; this was also reported in the most recent mullite spectra, and attributed to Al in sites of tetrahedral symmetry, but co-ordinated by only three oxygen atoms (sites designated as Al* [13]). The presence of the two tetrahedral resonances is more clearly revealed by fitting Gaussian peaks to the spectra (Fig. 4).

This procedure shows that at temperatures >1300 °C, the total proportion of tetrahedral Al remains essentially constant at about 58%; and of this, the proportion of trico-ordinated Al* also remains essentially constant at about 20–25% over this temperature range. The proportion of aluminium in tetrahedral environments is similar to the value for sintered synthetic mullite, estimated to be 52–53% from the published spectrum [13] obtained under identical conditions to the present work (11.7 T, spinning speed 12 kHz).

The X-ray powder pattern of halloysite heated at 1400 °C for 4 h indicates the presence of *x*-phase sialon, mullite and β′-sialon (Fig. 1). The reported ^{27}Al NMR spectra of *x*-phase sialon [19] and β′-sialon [21, 23] both contain octahedral and tetrahedral resonances of similar chemical shift to those of mullite (Table I), which may account for the apparent lack of change in the ^{27}Al NMR spectrum (Fig. 3d). However, the 4 h spectrum contains no evidence of the diagnostic β′-sialon peak at 103 p.p.m. [21, 23]; the reason for this is not clear, but is possible that the resonance in β′-sialon in its early stages of formation

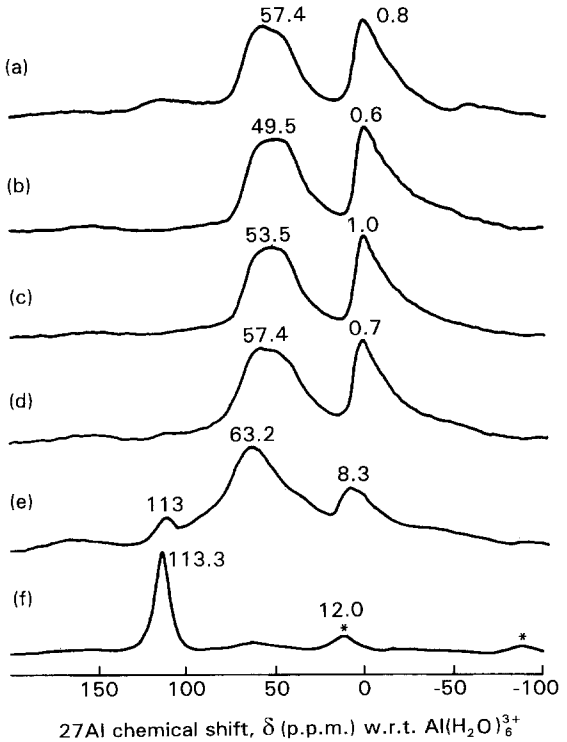

Figure 3 ^{27}Al MAS NMR spectra of halloysite–carbon mixtures fired in nitrogen at 1400 °C for: (a) 10 min, (b) 1 h, (c) 2 h, (d) 4 h, (e) 8 h, (f) 16 h. * Denotes spinning side band.

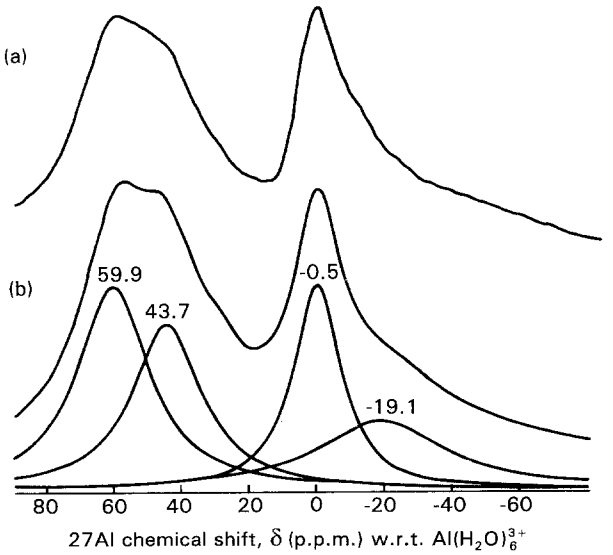

Figure 4 Peak fitting of a typical ^{27}Al MAS NMR spectrum (halloysite–carbon in nitrogen, 4 h at 1400 °C). (a) Observed spectrum, (b) spectrum synthesized from indicated peaks.

could be broadened beyond detection due to distortion in the Al sites bonded to nitrogen.

Heating at 1400 °C for 8 h causes a dramatic change in the ^{27}Al spectrum (Fig. 3e), with the appearance of a major new peak at 113 p.p.m., which is particularly strong in the kaolinite sample. Since peaks in this region are due to Al bonded to N, this is consistent with the appearance of significant concentrations of AlN in these samples. The presence of β′-sialon is indicated in both the kaolinite and halloysite samples by resonances at 64 and 4–8 p.p.m., in good agreement with published peak positions of 66 and 4 p.p.m. [18, 23]; the other β′-sialon peak at 103–109 p.p.m. could be masked by the broadness of the 113 p.p.m. peak of AlN. These spectra are broadly similar to those reported by Neal *et al.* [9].

After heating for 16 h, the intensities of the β′-sialon peaks at 64 and 4 p.p.m. are reduced almost to extinction in halloysite, but are still strongly present in kaolinite. The AlN resonance at 113 p.p.m. is strengthened in halloysite, in agreement with the X-ray trace of this sample. These results suggest that the intensity of the β′-sialon spectrum is much less than that of AlN, or, alternatively, there is considerably less β′-sialon in these samples than indicated by the X-ray data. Another important result is the apparent insensitivity of MAS NMR to the precursor sialon phases O′- and *x*-phase; these phases have Al resonances at about 48 and 62 p.p.m., coinciding with the two tetrahedral mullite resonances. The ^{27}Al NMR spectra of samples reacted for 2–4 h containing all three phases are essentially similar to less-reacted samples containing only mullite, even with respect to the relative proportions of the resonances at about 45 and 60 p.p.m. This lack of change in the Al spectra until the appearance at a late stage of AlN-type structures was attributed by Neal *et al.* [9] to a lack of participation by Al in the structure of the β′-sialon initially formed. Such an Al-free β′-sialon seems unlikely in view of the X-ray results for this phase as initially formed, which indicate *z*-values of approximately 1.8. An alternative, but related, explanation is that the Al content of the β′-sialon is initially associated with the oxygen structure, with well characterized Al–N bonds being formed only later in the reaction.

In summary, the usefulness of the ^{27}Al MAS NMR spectra in exploring the carbothermal reaction sequence is limited by their inability to distinguish between the various sialons and their precursor mullite phase, which all have resonances in the same general regions. The problem is compounded by the appearance of the diagnostic Al–N resonance relatively late in the reaction.

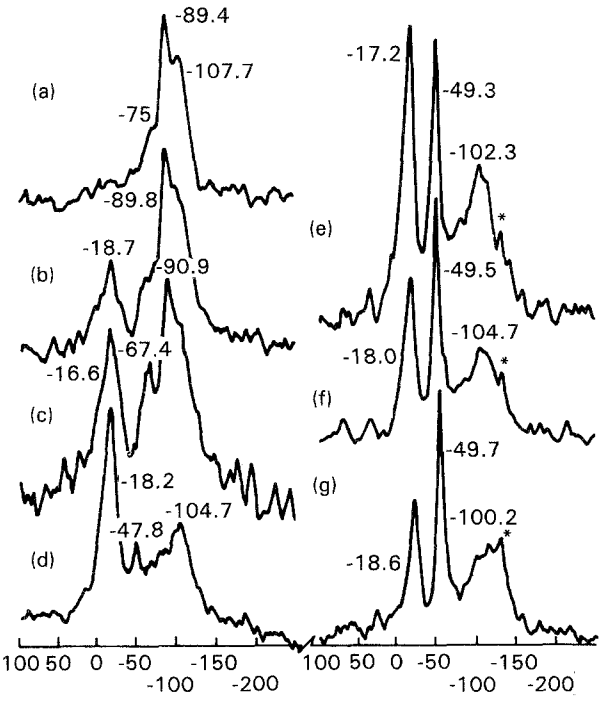

Figure 5 ^{29}Si MAS NMR spectra of kaolinite–carbon mixtures fired in nitrogen at 1400 °C for: (a) 10 min, (b) 1 h, (c) 2 h, (d) 4 h, (e) 8 h, (f) 12–16 h, (g) 24 h. * Denotes spinning side band.

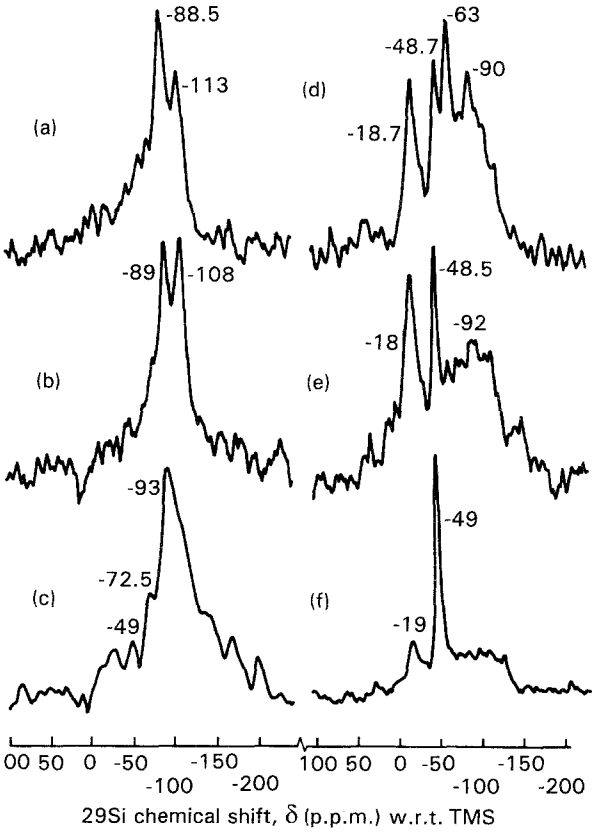

Figure 6 ^{29}Si MAS NMR spectra of halloysite–carbon mixtures fired in nitrogen at 1400 °C for: (a) 10 min, (b) 1 h, (c) 2 h, (d) 4 h, (e) 8 h, (f) 16 h.

3.2.2. ^{29}Si NMR

Typical ^{29}Si NMR spectra of kaolinite and halloysite heated with carbon in nitrogen at 1400 °C for varying times are shown in Figs 5 and 6, respectively.

The spectra of samples heated for up to 1 h contain two principal broad features; the resonance at −108 to −113 p.p.m. results from the silica which occurs as a by-product of mullite formation, and also from the cristobalite in the halloysite, which makes this chemical shift slightly more negative (Figs 5a and 6a). The ^{29}Si peak at about −89 p.p.m. is the principal mullite resonance [13]. The secondary mullite resonances at

−90 and −94.2 p.p.m. probably occur under the broad, unresolved mullite envelope. The peak at about −18 p.p.m. which is seen in kaolinite after 1 h firing (Fig. 5b) is diagnostic of SiC [14–17]; this peak appears in the halloysite samples only after firing for 2 h (Fig. 6c).

There is evidence of a very broad shoulder extending from about −60 to −80 p.p.m. (Fig 5a, b and 6c) which may arise from a continuum of silicon oxynitride species tending towards the more oxygen-rich compositions. After 2 h heating, this oxynitride resonance at −67.4 p.p.m. is more apparent, particularly in the kaolinite sample (Fig. 5c), and the mullite and silica resonances have been replaced by a very broad feature centred at −90 to −93 p.p.m. (Figs 5c and 6c), similar to a resonance sometimes observed in sialon precursors obtained by heating organometallic derivatives (M. R. Mucalo pers. comm.), and probably arising from an ill-defined mixture of largely silicon–oxygen compounds including elements of mullite structure, which is still strongly in evidence in the XRD traces of both kaolinite and halloysite. A similar ^{29}Si resonance was also found, together with a strong SiC resonance in the spectrum of the X-ray amorphous felt-like material deposited during sialon formation in the cool parts of the tube at the gas exit end; the Al in this material was almost exclusively tetrahedral ($\delta = 53.5$ p.p.m.). It is worth noting that the ^{29}Si NMR mullite resonance at −94.2 p.p.m. has been tentatively assigned to Si atoms in an environment influenced by the presence of trico-ordinated Al–O in distorted tetrahedral sites [13]; the development of this peak may, therefore, reflect the dominance of this type of Al/Si ordering as sialon formation proceeds.

The resonance which develops at −49 p.p.m. (Figs 5d and 6d) is common both to sialons and silicon nitride, but probably arises in these samples from the *x*-phase sialon which is seen by XRD to be at its maximum concentration (Fig. 2). After 4 h heating, SiC is strongly visible in both kaolinite and halloysite, in the broad resonance at −18 p.p.m. The other resonance at about −48 p.p.m. indicates a mixture of sialons (predominantly β′), while the persistence of more highly oxygenated phases is indicated by the broader peaks at about −90 to −104 p.p.m. These oxygenated species are present in kaolinite even after 24 h heating, but have disappeared from halloysite after 16 h heating (Fig. 6f).

In both kaolinite and halloysite heated for 16 h, a major phase visible in the NMR spectrum is β′-sialon, the resonance of which coincides with that of Si_3N_4 also known by XRD to be present in these samples. NMR indicates the presence of greater amounts of SiC and oxygenated Si species in kaolinite than in halloysite, suggesting that even after 24 h heating, the reaction in kaolinite has produced different products, possibly resulting from a different reaction path.

In summary, the ^{29}Si MAS NMR spectra complement the XRD view of the reaction sequence by providing the following additional information:

1. In the early stages of the reaction, the environment of the mullite silicon changes, adopting a range of local geometries which may, however, become increasingly dominated by the presence of oxygen vacancies.

2. At the same time, a range of silicon oxynitride compositions is formed, predominantly oxygen-rich, but possibly also containing small amounts of Al.

3. Long after the disappearance of mullite from the XRD record, traces of oxygenated silicon species are still detectable by NMR.

^{29}Si MAS NMR does not provide information about the following aspects of the reaction, which are best elucidated by XRD:

1. The final products (β′-sialon and β-silicon nitride) cannot be differentiated in these samples by NMR.

2. XRD appears to be more sensitive to the early presence of SiC, especially in kaolinite.

3.3. The pre-sialon reactions

As a part of this study of the structural factors influencing the formation of sialons at higher temperatures, the phases formed in the clays both in the presence and absence of carbon were investigated at temperatures between 1100–1400 °C. In this temperature range, the principal phase is mullite, with amorphous silica also distinguishable as a hump in the XRD trace. Below 1300 °C, the mullite is not sufficiently crystalline to make unit cell measurements, but above 1300 °C, the cell parameter is consistent with mullite containing about 60 mol % Al_2O_3, i.e. 3:2 mullite. The ^{27}Al NMR spectra are consistent with mullite (Fig. 4), and, as previously described, can be fitted by two tetrahedral peaks (regular 4-co-ordinated Al and Al*) and one octahedral peak. Fig. 7 shows the relative occupancy of these three sites as a function of temperature for halloysite, calculated from the relative intensities of the fitted peaks.

Fig. 7 shows that the presence of carbon has little effect on the formation of the Al* sites (δ =43–47 p.p.m.), nor on the octahedral Al sites (δ = −0.2–7.6 p.p.m.), which decrease in population as the Al* sites develop. In the presence of carbon, the "normal" 4-co-ordinated Al site population (δ =60–65 p.p.m.) remains unchanged; whereas in the absence of carbon, the population of these sites decreases in tandem with that of the octahedral sites (Fig. 7). Thus, the principal effect of carbon on the aluminium component is to promote the formation of a mullite with relatively more 4-co-ordinated Al and relatively less of the typical mullite-like Al*. The effect of this on subsequent sialon-forming reactions is unclear, since the proportions of both tetrahedral species remain approximately constant during sialon formation at 1400 °C.

The ^{29}Si NMR spectra of all the lower-temperature samples show the typical mullite and silica resonances. By fitting peaks to these spectra, the partitioning of Si between these phases can be calculated from the relative peak intensities. This indicates an increase in mullite at the expense of the silica with increasing temperature (Fig. 8).

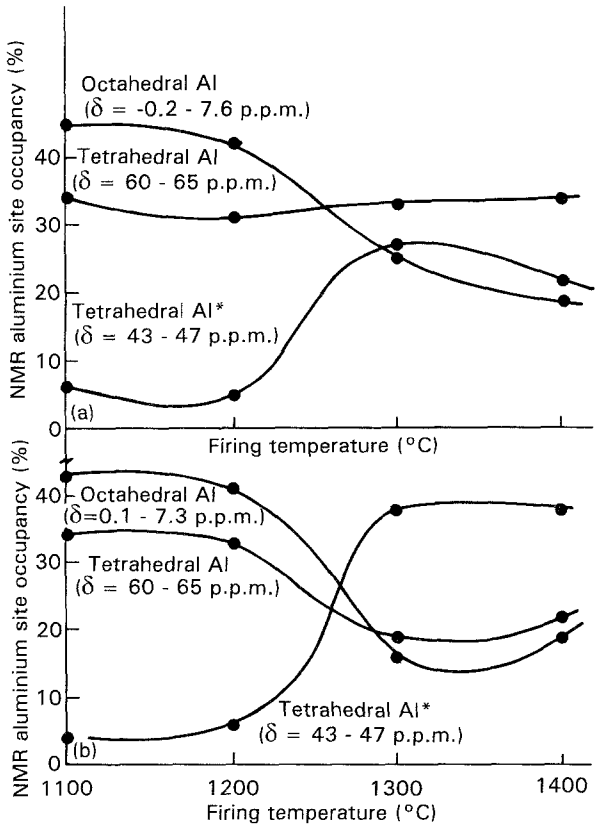

Figure 7 Relative site occupancy of Al in halloysite (a) with and (b) without carbon, fired in nitrogen at various temperatures, deduced from peak-fitted ^{27}Al MAS NMR spectra.

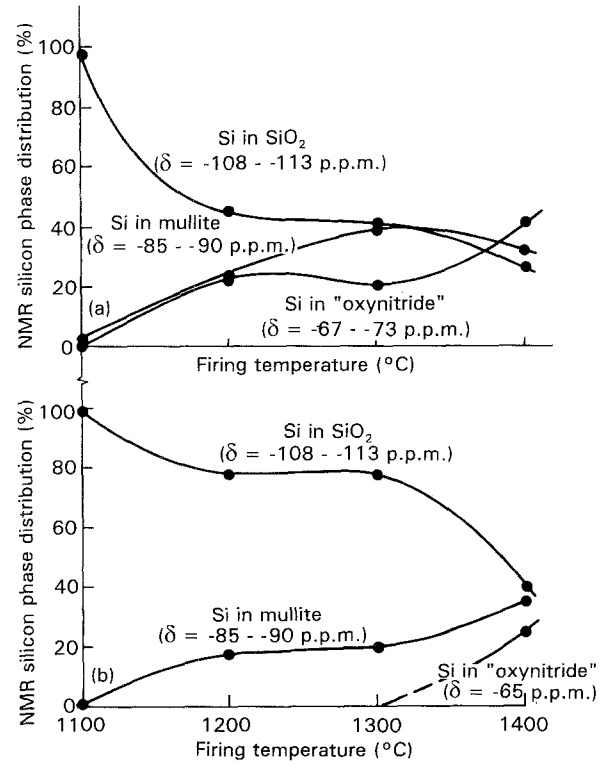

Figure 8 Relative Si content of various phases formed from halloysite (a) with and (b) without carbon, fired in nitrogen at various temperatures, deduced from peak-fitted ^{29}Si MAS NMR spectra.

Fig. 8 shows that the number of mullite-type silicon resonances formed with increasing temperature is essentially unaffected by the presence of carbon, but the loss of the SiO_2 resonances is significantly more marked in the presence of carbon. The balance of the Si in these samples occurs in a broad band centred at about −67 to −73 p.p.m., assigned provisionally to a continuum of silicon oxynitride species having a range of nitrogen contents. The presence of carbon apparently facilitates the formation of the necessary Si–N bonds at relatively low temperatures; a similar feature begins to appear in the carbon-free samples only at 1400 °C (Fig. 8b). Thus, the initial stages of sialon formation involve disruption of the silicon structure rather than the aluminium, with the formation of Si–N bonds which were hitherto unsuspected because they are not associated with crystalline phases. The formation of Si–C bonds, which has until now been postulated as occurring at an early stage in the reaction sequence, is detected by ^{29}Si NMR in these samples at a later stage, becoming visible in kaolinite and halloysite only after reaction at 1400 °C for 1 h and 2 h respectively (although X-ray diffraction suggests the presence of a small amount of SiC in kaolinite after 10 min reaction).

3.4. Implications for the reaction sequence

Both the NMR and complementary XRD results suggest, under the present reaction conditions, a more complex sequence of reaction intermediates and products than those previously suggested (Equations 1–4). The principal stages in the reaction (which can vary in sequence with the mineralogy of the reactant) can be approximately represented as follows:

1. Formation of mullite and amorphous silica:

$$3Al_2Si_2O_5(OH)_4 \rightarrow \underset{\text{mullite}}{3Al_2O_3 \cdot 2SiO_2} + 4SiO_2 + 6H_2O \quad (5)$$

2. Formation of silicon oxynitrides progressively richer in nitrogen, under the reducing influence of the carbon:

$$2SiO_2 + 3C + N_2 \rightarrow Si_2N_2O^* \quad (6)$$

3. Formation of x-phase sialon and β′-sialon from mullite:

$$2(\underset{\text{mullite}}{3Al_2O_3 \cdot 2SiO_2}) + 12C + N_2 \rightarrow \underset{x\text{-phase sialon}}{Si_3Al_6O_{12}N_5} + 6AlN + SiO_2 + 12C \quad (7)$$

$$\underset{x\text{-phase sialon}}{Si_3Al_6O_{12}N_2} + 3N_2 + 9C \rightarrow \underset{\beta'\text{-sialon}}{Si_3Al_3O_3N_5} + 2AlN + 9CO \quad (8)$$

4. Formation of SiC:

$$SiO_2 + 3C \rightarrow SiC + 2CO \quad (9)$$

* This phase may contain some aluminium (e.g. O′-sialon), suggesting that its origin is not solely amorphous silica as implied here.

5. Formation of Si_3N_4:

$$3SiO_2 + 6C + 2N_2 \rightarrow Si_3N_4^{\dagger} + 6CO \quad (10)$$

Under the present reaction conditions, the differences in the apparent sequence of these reactions in kaolinite and halloysite may arise from variations in the reactions, e.g. the earlier appearance of SiC and Si_3N_4 in the kaolinite samples may result from the formation of these phases in kaolinite directly from SiO_2 (Equations 9 and 10), rather than from x-phase sialon, as might occur in halloysite:

$$2Si_3Al_6O_{12} + 7N_2 + 27C \rightarrow Si_3N_4 + 3SiC + 12AlN + 24CO \quad (11)$$

The chief mineralogical difference between the present halloysite and kaolinite is the additional silica (cristobalite) in the former, which could react according to Equations 8 and 9. Cristobalite disappears after 4 h firing, by which time substantial SiC is detectable in the halloysite samples by NMR and XRD. By contrast, in kaolinite, which does not contain the additional silica, substantial SiC formation is detected by NMR after only 1 h, and even earlier by XRD. If the reasons for the differences between the kaolinite and halloysite are related to the additional silica, they are not clear from the present results.

4. Conclusions

Generally, the solid-state MAS NMR and X-ray diffraction data agree on the course of the reaction sequence involved in the carbothermal synthesis of sialons from kaolinite and halloysite. The two techniques provide complementary information; unlike XRD, ^{27}Al MAS NMR is not particularly helpful in distinguishing between the various sialon phases, because these have similar resonances which also coincide with the two tetrahedral resonances of the preceding mullite phase. A similar drawback is found with ^{29}Si MAS NMR, which cannot differentiate between β′-sialon and β-silicon nitride (both of which occur in the product assemblage, according to XRD).

However, MAS NMR provides information about aspects of the reaction which are not apparent from XRD, namely:

1. In the very early stages of the reaction (mullite formation) below 1300 °C, the presence of carbon in the reaction mixture leads to the formation of a lower concentration of trico-ordinated Al* sites associated with oxygen defects.

2. In the presence of carbon, the first Si–N bonds are formed at very low temperatures (1200 °C); these are initially associated with a range of non-crystalline oxynitride compositions which progressively become more nitrogen-rich. In the absence of carbon, the appearance of these phases is delayed until 1400 °C.

3. Si–O bonds persist in the reaction mixtures long after the disappearance of mullite, especially with kaolinite starting material. The chemical shift of these Si–O units suggests a configuration similar to Q^3 (tetrahedral silicate units with three bridging oxygens shared between two tetrahedra), with which Al may also be associated.

4. Si–C bonds appear later in the reaction sequence than would be expected from previous work (Equation 2). This is especially clear for halloysite, but even in kaolinite, in which a trace of SiC can be distinguished by XRD after 10 min reaction, the diagnostic ^{29}Si spectrum of SiC appears only after heating for 1 h. Under the present reaction conditions, SiC appears to behave more as a secondary product than a short-lived transitory intermediate.

5. The Al–N bonds are the last to form, appearing under the present conditions only after 8 h firing at 1400 °C, long after the detection of sialon phases by XRD. The absence of the diagnostic ^{27}Al resonance of β′-sialon suggests that at shorter reaction times, the Al–N portion of the β′-sialon is not established even though XRD indicated that the phase is present. At longer reaction times, the Al–N resonance of β′-sialon may be masked by the broader and more intense AlN resonance.

References

1. J. G. LEE and I. B. CUTLER, *Amer. Ceram. Soc. Bull.* **58** (1979) 869.
2. D. S. PERERA, *J. Aust. Ceram. Soc.* **23** (1987) 11.
3. M. E. BOWDEN, K. J. D. MACKENZIE and J. H. JOHNSTON, *Mater. Sci. Forum*, **34–36** (1988) 599.
4. J. B. BALDO, V. C. PANDOLFELLI and J. R. CASARINI, in Materials Science Monographs 16 (Ceramic Powders), edited by P. Vincenzini (Elsevier, Amsterdam, 1983), p. 437.
5. Y. SUGAHARA, K. KURODA and C. KATO, *J. Amer. Ceram. Soc.* **67** (1984) C247.
6. I. HIGGINS and A. HENDRY, *Proc. Brit. Ceram. Soc.* **38** (1986) 163.
7. M. E. BOWDEN, Private communication.
8. K. J. D. MACKENZIE, I. W. M. BROWN, R. H. MEINHOLD and M. E. BOWDEN, *J. Amer. Ceram. Soc.* **68** (1985) 293.
9. G. S. NEAL, M. E. SMITH, M. B. TRIGG and J. DRENNAN, in Proceedings of the International Ceramics Conference, Australia, 1992 (Austceram 92), Vol. 1, (Ed. M. J. Bannister, CSIRO, Melbourne, 1992), p. 533.
10. G. D. SORARU, A. RAVAGNI, R. CAMPOSTRINI and F. BABONNEAU, *J. Amer. Ceram. Soc.* **74** (1991) 2220.
11. J. M. THOMAS, J. KLINOWSKI, P. A. WRIGHT and R. ROY, *Angew Chem., Int. Ed. Engl.* **22** (1983) 614.
12. K. J. D. MACKENZIE, I. W. M. BROWN, R. H. MEINHOLD and M. E. BOWDEN, *J. Amer. Ceram. Soc.* **68** (1985) 266.
13. L. H. MERWIN, A. SEBALD, H. ROGER and H. SCHNEIDER, *Phys. Chem. Minerals* **18** (1991) 47.
14. J. S. HARTMAN, M. F. RICHARDSON, B. L. SHERRIFF and B. G. WINSBORROW, *J. Amer. Chem. Soc.* **109** (1987) 6059.
15. J. R. GUTH and T. PETUSKY, *J. Phys. Chem.* **91** (1987) 5361.
16. K. R. CARDUNER and R. O. CARTER III, *Ceram. Int.* **15** (1989) 327.
17. K. E. INKROTT, S. M. WHARRY and D. J. O'DONNELL, *Mater. Res. Symp. Proc.* **73** (1986) 165.
18. R. DUPREE, M. H. LEWIS, G. LENG-WARD and D. S. WILLIAMS, *J. Mater. Sci. Lett.* **4** (1985) 393.
19. J. KLINOWSKI, J. M. THOMAS, D. P. THOMPSON, P. KORGUL, K. H. JACK, C. A. FYFE and G. C. GOBBI, *Polyhedron* **3** (1984) 1267.

† This phase may also contain a little Al and, therefore, may not originate solely from amorphous SiO_2.

20. D. C. APPERLEY, M. E. A. CUDBY, R. K. HARRIS, G. L. MARSHALL, B. J. SAY, K. SMITH, D. P. THOMPSON and R. R. YEUNG, Poster No. 602, 8th International Meeting on NMR Spectroscopy, University of Kent, July 1987.
21. R. DUPREE, M. H. LEWIS and M. E. SMITH, *J. Appl. Cryst.* **21** (1988) 109.
22. N. D. BUTLER, R. DUPREE and M. H. LEWIS, *J. Mater. Sci. Lett.* **3** (1984) 469.
23. J. SJOBERG, R. K. HARRIS and D. C. APPERLEY, *J. Mater. Chem.* **2** (1992) 433.
24. W. E. CAMERON, *Amer. Ceram. Soc. Bull.* **56** (1977) 1003.

Received 11 June
and accepted 30 November 1993